Hindawi
Advances in Civil Engineering
Volume 2021, Article ID 1788691, 8 pages
https://doi.org/10.1155/2021/1788691

Research Article

Suppression of Bridge Flutter Using Suction Control

Shibo Tao

School of Civil Engineering, Jilin Jianzhu University, Changchun, Jilin, China

Correspondence should be addressed to Shibo Tao; taoshibo1985@163.com

Received 22 June 2021; Accepted 2 November 2021; Published 27 November 2021

Academic Editor: Meng Gao

To verify the effectiveness of the suction-based method for improving flutter stability of long-span bridges, the forced vibration experiments for extracting the flutter derivatives of a section model with and without suction were performed, and the corresponding critical flutter wind speeds of this structure were calculated out. It is shown by the experiment that the flutter stability of the bridge depends on suction configuration. As the suction holes locate at the leeward side of the model, the critical flutter wind speed can attain maximum under the same suction velocity. In the analytical results, it is remarkably effective that the suction control improves the long-span bridge flutter stability.

1. Introduction

With the current trend of increasing span of a bridge, the sensitivity of bridges to wind enhances dramatically. Therefore, in the design of long spanned bridges, flutter stability has to be carefully investigated so as not to excite the flutter oscillation below the designed wind velocity. Once flutter occurs, it will lead to collapse of structure totally. Therefore, how to improve the flutter stability of long-span bridges has been studied and concerned widely in the field of wind engineering. Generally, there are two methods employed for suppressing wind-induced vibration of long-span bridges, consisting of mechanical control measures and aerodynamic control measures [1–6]. Aerodynamic control measures include the passive aerodynamic approach and active aerodynamic approach. The former is a way of improving flow fields around the object indirectly, which can optimize the aerodynamic characteristics of an object by changing the structure shape, and the fluid boundary-layer structure is changed passively [7, 8]. A number of passive control methods have been proposed to reduce the drag, suppress the fluctuating lift, and manipulate the wake vortex shedding from circular cylinders, including surface protrusions, splitter plates, guiding vanes, and base-bleed [9]. The active aerodynamic approach improves wind flow characteristics around an object in a direct way [10]. Modi briefly reviewed developments in the exciting field of the moving surface boundary-layer control and suggested possible application in the next generation of civil engineering structures [11]. Kwon and Chang performed a full-bridge model experiment by attaching additional flaps directly to the edges of a deck model, and the results showed that this method could suppress structural flutter effectively [12]. In 2001, Wildel et al. conducted an experimental study on controlling pitching motion of a bridge deck with a trailing-flap method, and the results showed that this active aerodynamic method had a good effect on improving flow field around the model [13].

Suction is an active aerodynamic method, which controls wind flow around objects aerodynamically and is applied firstly in aviation. Scientists used the suction method in reducing drag and increasing lift force [14, 15], and it was confirmed to work well. The study on civil engineering structures is only just beginning in controlling wind-induced effects by this method. Xin et al. conducted numerical simulations to analyse the flutter stability of long-span bridges and the wind-induced static effects on structures with suction [16, 17]. Chen et al. used the suction-based flow control method to suppress the wake vortex shedding [18]. So far the experimental research studies on suppressing the flutter of long-span bridges by suction is still in the blank.

Therefore, based on the forced vibration method, a wind-tunnel test on the flutter stability of a long-span bridge with steady suction was carried out, and a section model of the Great Belt East Bridge was employed as the specimen. Comparing the critical flutter wind speed with and without suction, the effectiveness of improving long-span bridges flutter stability with the steady suction was verified.

2. Mathematical Model

2.1. Self-Excited Forces. The lift force and moment of the bridge section model in the two-dimensional flow field can be expressed in Scanlan's form with eight flutter derivatives, as follows [19]:

$$L = \frac{1}{2}\rho U^2 B\left[\left[KH_1^*(K)\frac{\dot{h}}{U} + KH_2^*(K)\frac{B\dot{\alpha}}{U} + K^2H_3^*(K)\alpha + K^2H_4^*(K)\frac{h}{B}\right], \tag{1a}$$

$$M = \frac{1}{2}\rho U^2 B^2\left[KA_1^*(K)\frac{\dot{h}}{U} + KA_2^*(K)\frac{B\dot{\alpha}}{U} + K^2A_3^*(K)\alpha + K^2A_4^*(K)\frac{h}{B}\right], \tag{1b}$$

where ρ is the density of the air; $B = 2b$ is the bridge deck width; U is the mean cross wind velocity; $\boldsymbol{h}$ and $\boldsymbol{\alpha}$ are the respective vertical and torsional displacements; and each dot denotes a derivative with respect to time; L and M are the self-excited lift force and moment, respectively; $K=B\omega/U$ is the nondimensional reduced frequency; ω is the circular frequency oscillation. The nondimensional aerodynamic coefficients $A_i^*$and H_i^* $(i = 1\text{–}4)$ are called the flutter derivatives, and they evolve as functions of the reduced velocity U/fB, where $f = \omega/2\pi$ is the frequency oscillation.

Flutter instability of structures can be assessed analytically using the flutter derivative formulation, and a set of flutter derivative coefficients is used for this purpose. These coefficients can be determined from wind-tunnel experiments on the section model excited by initial displacements.

2.2. Extract the Flutter Derivatives of a Bridge Section. The motion differential equation of the system with two degrees of freedom is as follows:

$$m\left(\ddot{h} + 2\zeta_h\omega_h\dot{h} + \omega_h^2 h\right) = L, \tag{2a}$$

$$I\left(\ddot{\alpha} + 2\zeta_\alpha\omega_\alpha\dot{\alpha} + \omega_\alpha^2\alpha\right) = M, \tag{2b}$$

in which m means the unit length quality; I means the unit length inertia; and ζ means the mechanical damping ratio.

For the purpose of extraction the flutter derivatives, according to the demand of the forced vibration test in a wind tunnel, a sinusoidal motion of a bridge section model is forced to execute, and the single vertical and single rotational movement states (displacement and velocity) at a definite time instant can be expressed as follows:

$$h(t) = h_0\sin(\omega_h t), \tag{3a}$$

$$\dot{h}(t) = \omega_h h_0\cos(\omega_h t), \tag{3b}$$

$$\alpha(t) = \alpha_0\sin(\omega_\alpha t), \tag{3c}$$

$$\dot{\alpha}(t) = \omega_\alpha\alpha_0\cos(\omega_\alpha t), \tag{3d}$$

in which $h_0$and $\alpha_0$represent the vertical and rotational vibration amplitudes, respectively, and t is the time. Equations (3a) and (3b) are referred as the single vertical motion and equations (3c) and (3d) as the single rotational motion, respectively. Two series of motions make the aerodynamic forces uncoupled. The above four equations give the wall boundary conditions for the bridge model in wind inflow.

When the single vertical motion of a bridge model was performed, equations (1a) and (1b) taking an uncoupled form are rewritten as follows:

$$L = \frac{1}{2}\rho U^2 B\left[KH_1^*(K)\frac{\dot{h}}{U} + K^2H_4^*(K)\frac{h}{B}\right], \tag{4a}$$

$$M = \frac{1}{2}\rho U^2 B^2\left[KA_1^*(K)\frac{\dot{h}}{U} + K^2A_4^*(K)\frac{h}{B}\right]. \tag{4b}$$

Once the aerodynamic forces are established, the critical conditions for the onset of aerodynamic instability can be calculated. Consider the definite states at n discrete time instants in a complete time period of the model vibration, so that equations (3a) and (3b) are written in matrix style as

$$F = CX, \tag{5}$$

where

$$F = \{L_i \;\; M_i\}^T \quad i = 1 \sim n, \tag{6a}$$

$$X = \{H_1^* \;\; H_4^* \;\; A_1^* \;\; A_4^*\}^T, \tag{6b}$$

with C the corresponding coefficients matrix. Then, the aerodynamic derivatives are obtained as follows:

$$X = \left(C^TC\right)^{-1}CF. \tag{7}$$

The other flutter derivatives can also be obtained in the same way. The solution of the flutter equations can be obtained if plots of the flutter derivatives H_i^* and A_i^* are available from measurements as functions of K. Then, the flutter speed can be calculated.

The flutter speed $U_{cr} = B\omega_{cr}/K$, wherein ω_{cr} is the flutter frequency. The critical wind speed U_{cr} is the lowest possible

wind speed resulting in the aeroelastic instability. For the purpose of practical flutter prediction, the critical wind speed U_{cr} is the most important factor and of concern. The flutter frequency does not coincide with the natural frequencies of the structure as the dynamic properties are modified by the self-excited forces.

3. The Forced Vibration Experiment of a Bridge Flutter with Suction

3.1. Test Model. A 1 : 40 geometrically scaled section model of the Great Belt East Bridge was adopted. The model is 775 mm wide (B), 110 mm deep (D), and 1200 mm long (L) (see Figure 1). The mass of the bridge model is 11 kg (9.2 kg/m). The blockage ratio of the experiment facility was about 2.2%, and it was unnecessary to correct the data for the blockage effect [20]. The bridge situated in Denmark comprises a 1624 m main-span suspension bridge flanked by two continuous multispan approach bridges. The experimental study was performed at Re 10^4. And the Great Belt East bridge Reynolds numbers are about 10^5~10^6. Therefore, there are two orders of magnitude difference between section model and prototype Reynolds numbers.

The suction hole is circular and 0.7 cm in diameter, and there are 7 columns 28 suction holes in total arranged on the undersurface of the model.

Figure 2 shows that each column stands for one suction configuration, from left to right, which denoteK_1, K_2, K_3, K_4, K_5, K_6, and K_7. Every suction configuration has four suction holes, which are opened while the other holes shut off.

Suction control works through suction flow, which is generated by a specialized apparatus installed on an object surface. The suction flow generated from external energy supply may improve wind field characteristics around an object so as to reduce wind-induced effects on the object. Steady suction refers that the velocity of suction remains constant at each moment. Its parameters mainly include suction velocity and suction coefficient.

Here, we define the suction coefficient C_s as

$$C_s = \frac{VS_s}{US_d}, \tag{8}$$

in which V is suction velocity; S_s is area of suction hole; and S_d is undersurface area of the model. In the test, $S_d = 0.57\ \mathrm{m}^2$.

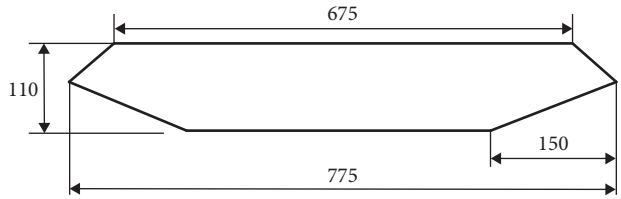

Figure 1: The deck cross section (unit: mm).

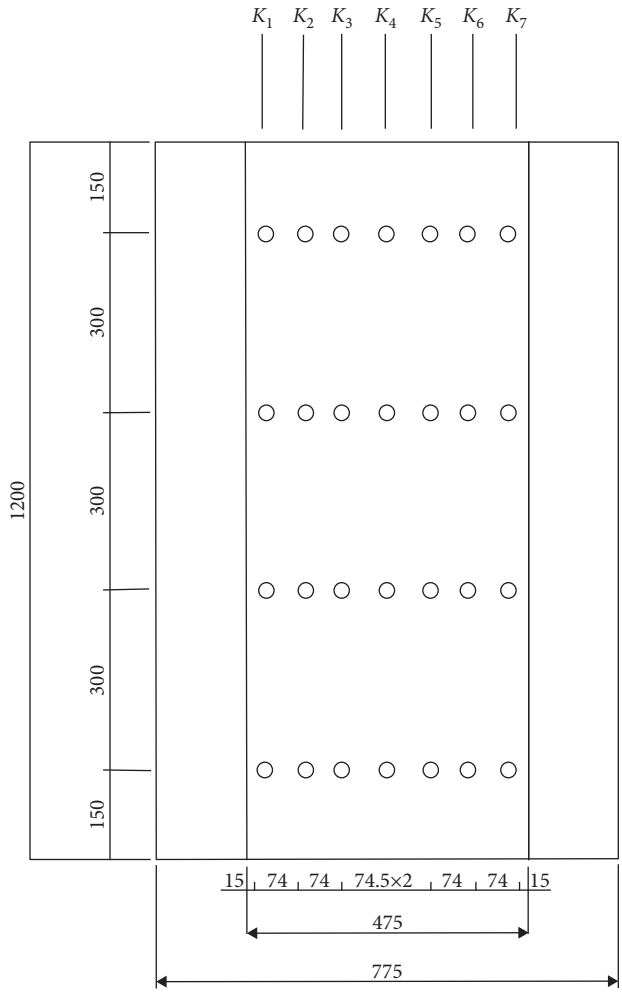

Figure 2: Undersurface of the model (unit: mm).

3.2. Experimental Device. The forced vibration test for flutter derivatives extraction was conducted in the atmospheric boundary-layer wind tunnel. The wind tunnel is a closed-circuit tunnel with a rectangular test section that is 4 m wide, 3 m high, and 25 m long. The wind speed (U) is continuously variable, and the flow has a longitudinal turbulence intensity of less than 0.46%. The performance parameters of the forced vibration system are given in Table 1. Two Omega160 IP60 version six-axis force sensors are used in the test. The sensors are produced by American ATI Company. They can measure all three forces (drag, lift, and side forces) and three moments (yaw, pitch, and roll moments). The forces capacity is ±1000 N, and the resolution is 0.25 N. The moment capacity is ±120 N·m in the measuring, and its resolution is 0.0125 N, whose full-scale error is 0.5% equivalent to 5 N. The accelerometers adopted are Type 4507B produced by Danish B&K Company. The amplitude frequency range of the accelerometer is 0.3 Hz–6 kHz. Four accelerometers are mounted on the four corners of the undersurface of the model.

In this test, the section model was given vertical amplitude of 14 mm and torsional amplitude of 3°, and the frequencies of two motions in vertical and torsional were both 0.5 Hz. The acceleration measurements were obtained by acquiring data at a sampling frequency of 100 Hz for a

Table 1: Performance parameters of the forced vibration system.

System span: 4000 mm Frequency:0–5 Hz
Range of angle of attack: from −15° to +15° Resolution of angle of attack: 1°Vertical amplitude: 4 mm–30 mm Lateral amplitude: 4 mm–30 mm Torsional amplitude: 1°–10° Style: sinusoidal motion

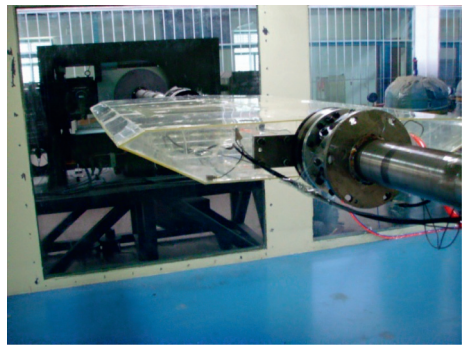

Figure 3: Section model and forced vibration system.

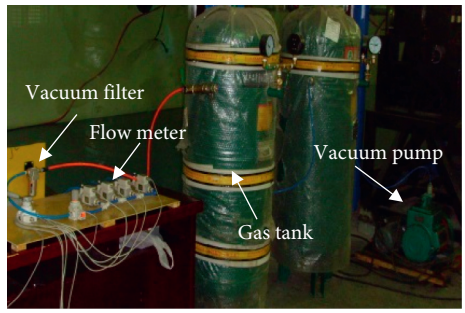

Figure 4: Suction system.

Figure 5: Flow meter.

period of 20 s. And the forces measurement data were acquired for 20 s at a data acquisition rate of 100 Hz. Besides, the angle of attack $_{\alpha}$ was 0°. A connection graph for the section model and the forced vibration system is shown in Figure 3.

3.3. Suction System. The suction system mainly consists of four parts: the air source system, the gas source processing system, the pipe network, and the control system. The suction system in the experiment is shown in Figure 4.

Four flow meters are used in the test. The flow meters are produced by Chinese SMC Company, as shown in Figure 5.

4. Results and Analysis

4.1. Flutter Derivatives. All the eight flutter derivatives of the section model obtained with and without suction are plotted in Figure 6. The forced vibration method was used to extract the flutter derivatives [21–23]. K_0 means no suction.

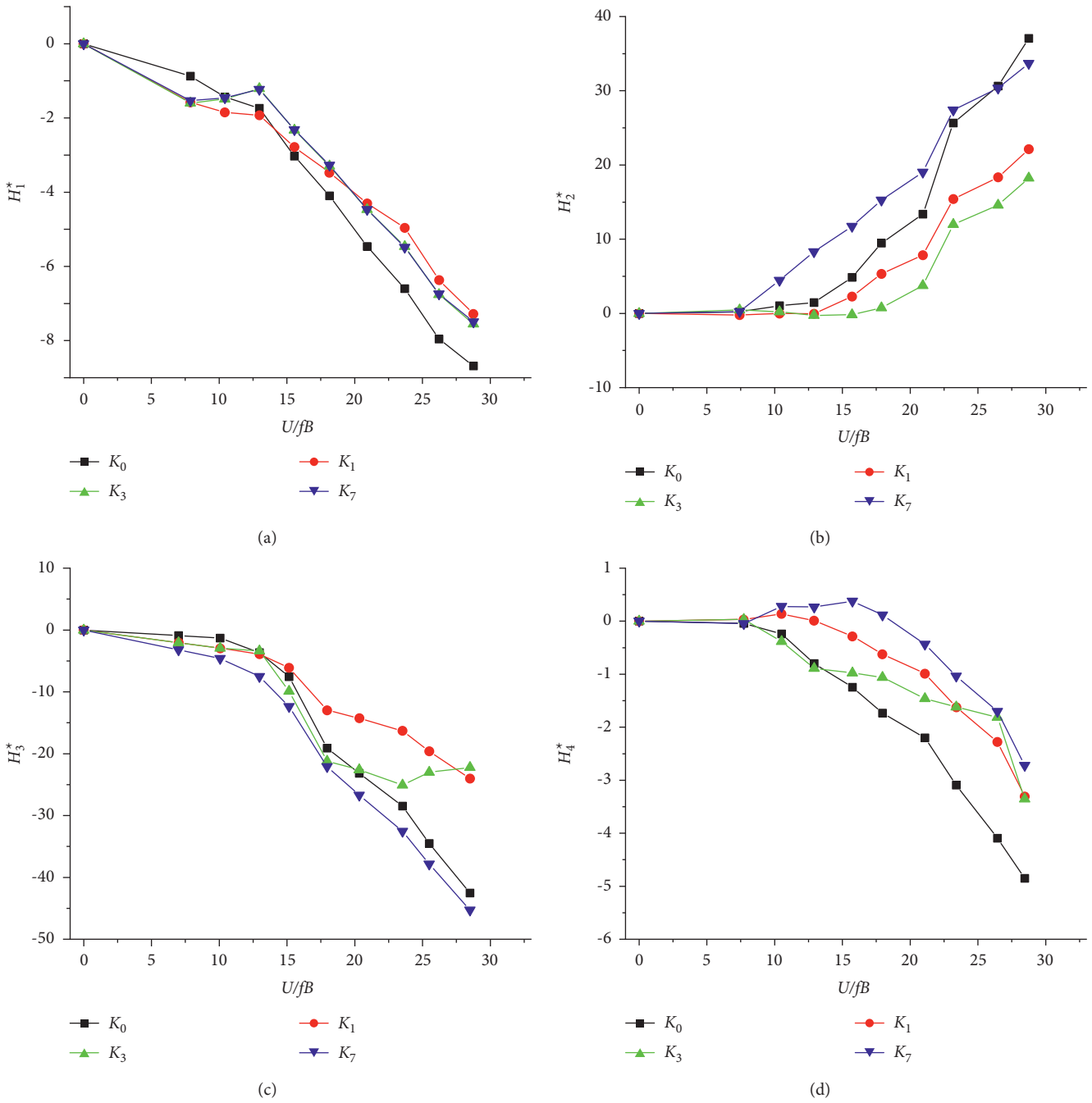

Figure 6: Continued.

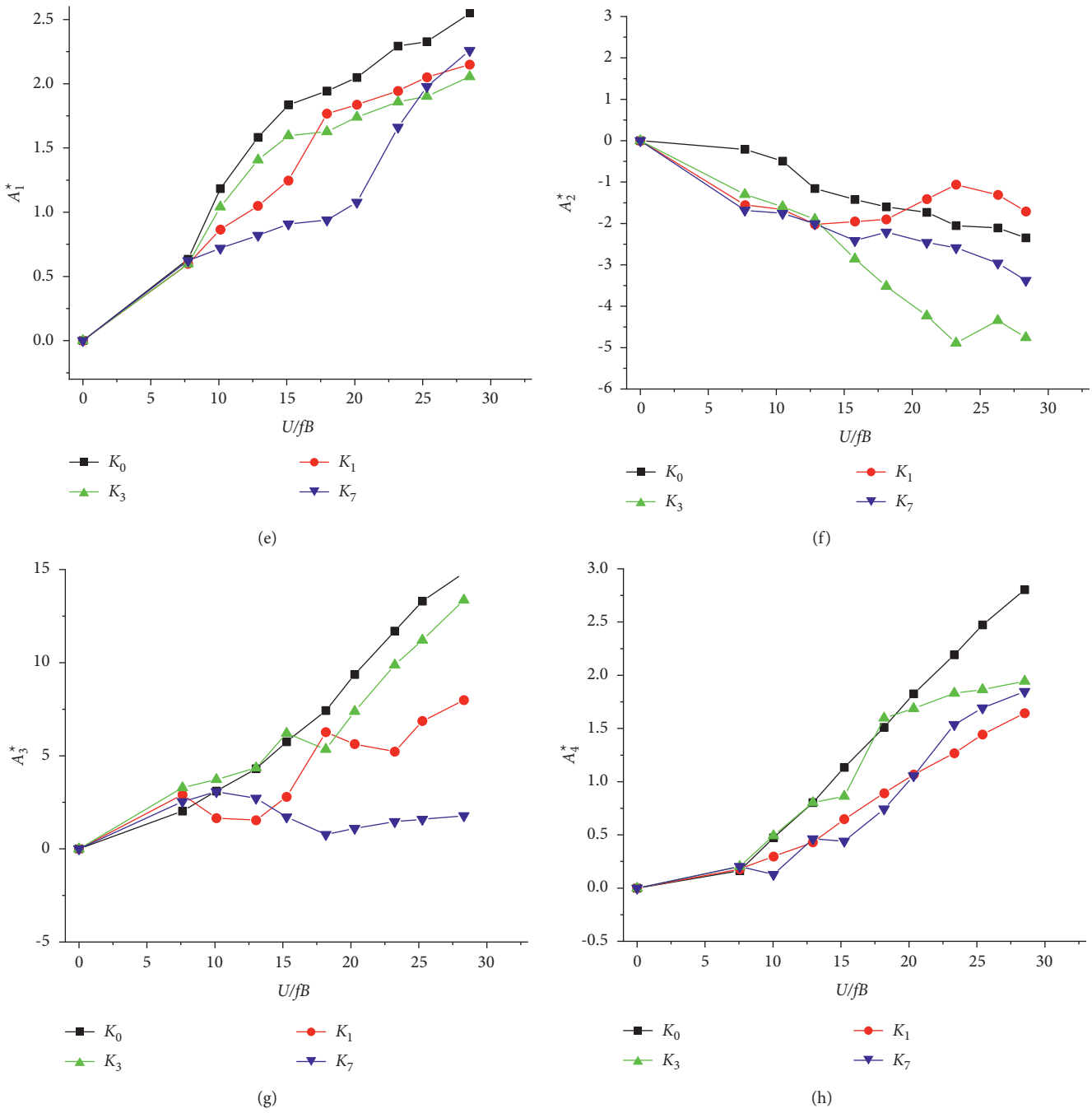

Figure 6: Flutter derivatives (Cs = 0.0018): (a) H_1*; (b) H_2*; (c) H_3* (d) H_4*; (e) A_1*; (f) A_2*; (g) A_3*; (h) A_4*.

In Figure 6, all the derivatives show a lot of variations in different suction configurations and no suction with increasing the reduced wind speed. In Figure 6(b), with suction control, the A_3^* is significantly reduced, especially for K_7 suction configuration. It can be seen from equation (1b) that A_3^* reflects the relationship between torsional displacement and pitching moment. Therefore, the aerodynamic pitching moment of the bridge is affected by suction in the process of torsional displacement.

4.2. Flutter Critical Frequency and Wind Speed. Table 2 shows the structural parameters of the bridge.

As the flutter derivatives and the structural parameters shown in Table 2, the flutter critical frequency and wind speed of this bridge in different suction are achieved as shown in Table 3.

In Table 3, the flutter critical wind speed is 38.8 m/s without suction; the flutter critical wind speed is 52.7 m/s with K_1 suction configuration; the flutter critical wind speed is 50.8 m/s with K_3 suction configuration; and the flutter critical wind

Table 2: Data of structural parameters of the bridge.

Property	Symbol	Value	Unit
Unit length quality	M	17.8×103	kg/m
Unit length rotational inertia	I	2.173×106	kg·m
Frequency in vertical direction	Fh	0.099	Hz
Frequency in torsional direction	Fα	0.186	Hz
Damping ratio in vertical direction	Zh	0.0	—
Damping ratio in torsional direction	Zα	0.0	—

Table 3: Flutter critical frequency and wind speed.

Suction configuration	$K0$	$K1$	$K3$	$K7$
ωcr (rad/s)	0.3142	0.4398	0.4084	0.5027
Ucr (m/s)	38.8	52.7	50.8	65.8

speed is 65.8 m/s with K_7 suction configuration. Therefore, the flutter critical wind speed is increased with suction control. And when the suction position is located at the bottom of the bridge far away from the incoming wind end, the effects of the suction control are the best for improving the flutter stability. The possible reason is that suction control can restrain boundary-layer separation so as to suppress the flutter of the bridge.

5. Conclusions

This paper proposes the suction control to suppress flutter of the long-span bridge. The forced vibration experiment of the section model was performed with the steady suction. The main conclusions can be drawn as follows:

(1) The suction control has influence on the flutter derivatives, especially for $A_3{}^*$. $A_3{}^*$ is significantly reduced, for K_7 suction configuration. Therefore, the aerodynamic pitching moment of the bridge is affected by suction in the process of torsional displacement.

(2) The suction control can improve the flutter stability of a long-span bridge; when the suction position is located at the bottom of the bridge far away from the incoming wind end, the effects of the suction control are the best for improving the flutter stability. And the possible reason is that suction control can restrain boundary-layer separation so as to suppress the flutter of the bridge.

Data Availability

The data used in this study are available from the corresponding author upon request.

Conflicts of Interest

The author declares that there are no conflicts of interest regarding the publication of this paper.

Acknowledgments

The authors would like to thank BIAN Xiao-xian and Engineer ZHAO Peng for their help during the preparation of the tests and for their efforts during the tests.

References

[1] P. Duc-Huynh and K. Hiroshi, "An experimental study of flutter and buffeting control of suspension bridge by mechanically driven flaps," *Wind and Structures*, vol. 14, no. 2, pp. 153–165, 2011.

[2] L. Y. Wang, "Mitigation of wind-rain-induced cable vibration in cable-stayed bridges: measurement error," *Applied Mechanics and Materials*, vol. 226-228, pp. 1630–1633, 2012.

[3] L. Y. Wang and Y. L. Xu, "Active stiffness control of wind-rain-induced vibration of prototype stay cable," *International Journal for Numerical Methods in Engineering*, vol. 74, no. 1, pp. 80–100, 2010.

[4] R. Santoro and G. Failla, "An interval framework for uncertain frequency response of multi-cracked beams with application to vibration reduction via tuned mass dampers," *Meccanica*, vol. 56, no. 1, pp. 923–952, 2021.

[5] V. B. Patil and R. S. Jangid, "Optimum multiple tuned mass dampers for the wind excited benchmark building/omsvvap," *Journal of Civil Engineering and Management*, vol. 17, no. 4, pp. 540–557, 2011.

[6] T. Bandivadekar and R. Jangid, "Optimization of multiple tuned mass dampers for vibration control of system under external excitation," *Journal of Vibration and Control*, vol. 19, no. 12, pp. 1854–1871, 2013.

[7] F. Xie and A. M. Aly, "Structural control and vibration issues in wind turbines: a review," *Engineering Structures*, vol. 10, pp. 110087.1–110087.28, 2020.

[8] A. V. Kuznetsov and D. A. Nield, "The Cheng-Minkowycz problem for natural convective boundary layer flow in a porous medium saturated by a nanofluid: a revised model," *International Journal of Heat and Mass Transfer*, vol. 65, pp. 682–685, 2013.

[9] W.-L. Chen, D.-L. Gao, W.-Y. Yuan, H. Li, and H. Hu, "Passive jet control of flow around a circular cylinder," *Experiments in Fluids*, vol. 56, no. 11, p. 201, 2015.

[10] R. C. Battista and M. S. Pfeil, ""Control of wind oscillations of Rio-Niteroi bridge," Brazil," *Proceedings - Institution of Civil Engineers*, vol. 163, no. sb2, pp. 87–96, 2010.

[11] V. J. Modi, "Moving surface boundary-layer control: a review," *Journal of Fluids and Structures*, vol. 11, no. 6, pp. 627–663, 1997.

[12] S.-D. Kwon and S.-P. Chang, "Suppression of flutter and gust response of bridges using actively controlled edge surfaces," *Journal of Wind Engineering and Industrial Aerodynamics*, vol. 88, no. 2-3, pp. 263–281, 2000.

[13] K. Wilde, P. Omenzetter, and Y. Fujino, "Suppression of bridge flutter by active deck-flaps control system," *Journal of Engineering Mechanics*, vol. 127, no. 1, pp. 80–89, 2001.

[14] X. Han and S. Krajnović, "Large eddy simulation of flow control around a cube subjected to momentum injection," *Flow, Turbulence and Combustion*, vol. 92, no. 1-2, pp. 527–542, 2014.

[15] H. Harinaldi, B. Budiarso, Warjito et al., "Modification of flow structure over a van model by suction flow control to reduce aerodynamics drag," *MAKARA of Technology Series*, vol. 16, no. 1, pp. 15–21, 2012.

[16] D. B. Xin, J. P. Ou, H. Li, and Z. -H. Li, "Suppression method for wind-induced flutter of long-span bridge based on steady air-suction," *Journal of Jilin University (Engineering and Technology Edition)*, vol. 41, no. 5, pp. 1273–1278, 2011, in Chinese.

[17] D. B. Xin, M. J. Zhang, J. P. Ou, and H. Li, "The method of steady air-suction used to improve the wind-induced static

effect on a slab," *Chinese Journal of Computational Mechanics*, vol. 29, no. 3, pp. 452–457, 2012, in Chinese.

[18] W.-L. Chen, D.-B. Xin, F. Xu, H. Li, J.-P. Ou, and H. Hu, "Suppression of vortex-induced vibration of a circular cylinder using suction-based flow control," *Journal of Fluids and Structures*, vol. 42, pp. 25–39, 2013.

[19] R. H. Scanlan and J. J. Tomko, "Airfoil and bridge deck flutter derivatives," *Journal of Engineering Mechanics, ASCE*, vol. 97, no. 6, pp. 1171–1737, 1971.

[20] F. Gu, J. S. Wang, X. Q. Qiao, and Z. Huang, "Pressure distribution, fluctuating forces and vortex shedding behavior of circular cylinder with rotatable splitter plates," *Journal of Fluids and Structures*, vol. 28, pp. 263–278, 2012.

[21] P. Leyland, V. Carstens, F. Blom, and T. Tefy, "Fully coupled fluid-structure algorithms for aeroelasticity and forced vibration unduced flutter: applications to compressor cascade," *Revue Europenne Des lments Finis*, vol. 9, no. 6, pp. 763–803, 2000.

[22] H. Niu and Z. Chen, "Three degrees-of-freedom forced vibration method for identifying eighteen flutter derivatives of bridge decks," *China Civil Engineering Journal*, vol. 47, no. 4, pp. 75–83, 2014.

[23] A. Cigada, M. Falco, and A. Zasso, "Development of a new system to measure aerodynamic forces on section models in wind tunnel testing," *Wind Engineering and Industrial Aerodynamics*, vol. 89, no. 7-8, pp. 725–746, 2001.